frontiers | Frontiers in Materials

TYPE Original Research
PUBLISHED 05 December 2023
DOI 10.3389/fmats.2023.1229036

OPEN ACCESS

EDITED BY
Peide Ye,
Purdue University, United States

REVIEWED BY
Nicolò Zagni,
University of Modena and Reggio Emilia, Italy
Lakshmi Narayanan Mosur Saravana Murthy,
Intel, United States

*CORRESPONDENCE
Srabanti Chowdhury,
srabanti@stanford.edu

RECEIVED 25 May 2023
ACCEPTED 16 November 2023
PUBLISHED 05 December 2023

CITATION
Lee KJ, Wen X, Nakazato Y, Chun J, Noshin M, Meng C and Chowdhury S (2023), A systematic study on the efficacy of low-temperature GaN regrown on *p*-GaN to suppress Mg out-diffusion. *Front. Mater.* 10:1229036. doi: 10.3389/fmats.2023.1229036

A systematic study on the efficacy of low-temperature GaN regrown on *p*-GaN to suppress Mg out-diffusion

Kwang Jae Lee[1], Xinyi Wen[1], Yusuke Nakazato[1], Jaeyi Chun[1], Maliha Noshin[1], Chuanzhe Meng[1,2] and Srabanti Chowdhury[1]*

[1]Department of Electrical Engineering, Stanford University, Stanford, CA, United States, [2]Department of Materials Science and Engineering, Stanford University, Stanford, CA, United States

Embedding *p*-type gallium nitride (*p*-GaN) in $Al_xGa_{1-x}N$-based thin films has garnered significant interest as a versatile structure for bandgap engineering such as tunnel/super-junctions or current blocking/guiding functions in electronic devices. However, Mg, a *p*-GaN dopant, has an undesirable diffusive capacity into the nearby thin films at a high growth temperature (>1,000°C), resulting in structural challenges in device design. This study systematically investigated the low-temperature GaN (LT-GaN) layer regrown on *p*-GaN that suppresses Mg diffusion according to metal–organic chemical vapor deposition growth conditions. Prototype $Al_{0.3}Ga_{0.7}N$ (40 nm)/GaN (140 nm) high-electron-mobility transistors (HEMTs) were regrown with LT-GaN on *p*-GaN (300 nm), and a high two-dimensional electron gas (2DEG) density of 3.13E12 cm^{-2} was achieved by inserting a 100-nm-thick LT-GaN layer grown at 750°C; in contrast, only 1.76E10 cm^{-2} 2DEG density was obtained from $Al_{0.3}Ga_{0.7}N$/GaN HEMTs regrown directly on *p*-GaN (Mg: 4.0E19 cm^{-3}). The fabricated $Al_{0.3}Ga_{0.7}N$/GaN HEMTs with 100-nm-thick LT-GaN demonstrated a high drain current density of 84.5 mA/mm with a low on-state resistance of 31 Ω·mm. The $Al_xGa_{1-x}N$/LT-GaN/*p*-GaN platform demonstrated here paves the way for various III-nitride-based structures with embedded *p*-GaN.

KEYWORDS

pulsed low-temperature growth, Mg diffusion, MOCVD thin-film growth, AlGaN/GaN HEMT, power electronics

1 Introduction

Gallium nitride (GaN) has attracted a great deal of attention as a next-generation power electronic material to replace silicon (Si) due to its excellent characteristics such as high electron mobility and high breakdown field (Chowdhury et al., 2013; Chowdhury and Mishra, 2013). In general, GaN thin films are grown using a metal–organic chemical vapor deposition (MOCVD) system, and Mg doping for *p*-type GaN (*p*-GaN) remains as a last step on the top of epitaxial layers due to the large diffusivity of Mg from the *p*-GaN surface and the reactor wall of MOCVD (Ran et al., 2006). Evidently for the Ga-polar *p*-GaN thin-film growth (Benzarti et al., 2008), these residual Mg dopants unintentionally diffuse into $Al_xGa_{1-x}N$-based thin films that are regrown on *p*-GaN, even though Mg source (Cp_2Mg) injection into a reactor was ceased (Fichtenbaum et al., 2008). Nevertheless, embedding *p*-GaN has recently emerged as an important research topic to create more efficient and

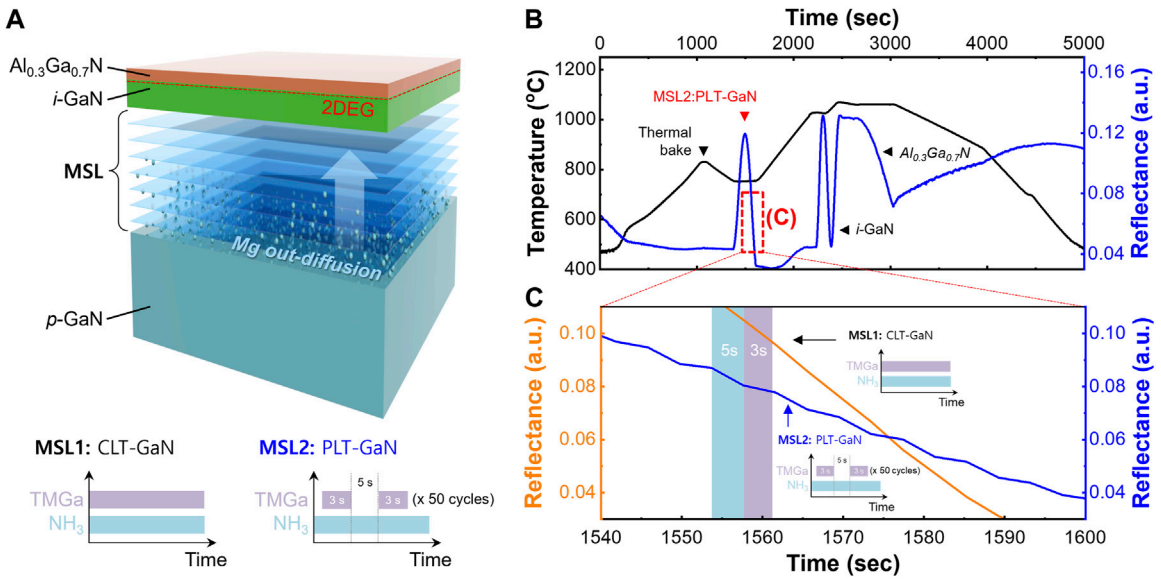

FIGURE 1
(A) Schematic structure of $Al_{0.3}Ga_{0.7}N$/*i*-GaN with LT-GaN MSLs regrown on *p*-GaN. Two types of the MSLs with and without perturbation (or pulsed injection) of a TMGa metal–organic source were introduced: the TMGa source for the MSL growth was injected in a continuous form (CLT-GaN) or a pulsed form (PLT-GaN). **(B)** *In situ* reflectance and growth temperature during the MOCVD process for $Al_{0.3}Ga_{0.7}N$/*i*-GaN/PLT-GaN thin-film regrowth. **(C)** The part of the PLT-GaN growth step in Figure 2B is shown enlarged, where two different growth rates repeated 50 times can be observed in one cycle: (i) TMGa interruption step (5 s) and (ii) TMGa injection step (3 s).

higher-performance electronic devices, e.g., lateral AlGaN/GaN high-electron-mobility transistors (HEMTs) including a *p*-GaN buffer layer (Lee et al., 2014), vertical super-junction metal-oxide-semiconductor field-effect transistors (MOSFETs) using a field-stop *p*-GaN layer (Xiao et al., 2019; Zhou et al., 2019), and current aperture vertical electron transistors (CAVETs) with a current blocking *p*-GaN layer (Chowdhury et al., 2008; 2011).

To date, various solutions have been suggested to suppress Mg out-diffusion such as *ex situ* wet chemical treatment using hydrofluoric acid (Xing et al., 2003), the *in situ* dry etching process with H_2 carrier gas (Soman et al., 2019), alternative regrowth using molecular beam epitaxy (MBE) instead of using MOCVD (Chowdhury et al., 2011; Brown et al., 2013; Wu et al., 2021), and the introduction of low-temperature aluminum nitride (LT-AlN) or LT-GaN insertion layers as an Mg suppression layer (MSL) (Tomita et al., 2008; Agarwal et al., 2017). Agarwal et al. (2017) recently reported the LT flow-modulated epitaxy (referred to as pulsed LT-GaN) technique for high crystallinity of intrinsic GaN (*i*-GaN) regrown on *p*-GaN with improved surface morphology as well as suppression of Mg out-diffusion. As the demand for embedding *p*-GaN in the $Al_xGa_{1-x}N$ thin film without Mg diffusion increases explosively, it is also important to explore the characteristics of MSLs through an electronic device embedding *p*-GaN.

In this study, we systematically investigate the efficacy of LT-GaN regrown on *p*-GaN as the MSL and its dependence on MOCVD growth conditions. Two types of MSL with and without perturbation (or pulsed injection) of a trimethylgallium (TMGa) metal–organic source were employed to investigate Mg out-diffusion: (1) an MSL with a continuous injection (CLT-GaN) and (2) an MSL with a pulsed injection (PLT-GaN) of the TMGa source. Subsequently, $Al_{0.3}Ga_{0.7}N$ (40 nm)/*i*-GaN (140 nm) thin films for prototype HEMTs were regrown on MSLs to explore the decay rate of Mg diffusion and the two-dimensional electron gas (2DEG) characteristics. Secondary ion mass spectrometry (SIMS) depth profiles were measured to analyze the Mg diffusion into regrown $Al_{0.3}Ga_{0.7}N$/*i*-GaN according to the MOCVD growth condition of LT-GaNs. Capacitance–voltage (*C*–*V*) and current–voltage (*I*–*V*) measurements were also taken to understand 2DEG and the output/transfer characteristics of $Al_{0.3}Ga_{0.7}N$/*i*-GaN HEMTs with our LT-GaN MSLs. This work demonstrates the importance of suppressing Mg out-diffusion in device performance and shows the correlation between the degree of Mg diffusion and 2DEG density according to various growth conditions of existing LT-GaN.

2 Experimental procedure

A 300-nm-thick *p*-GaN and 3 μm-thick *i*-GaN buffer layer were grown at 930°C and 1,040°C, respectively, by using the MOCVD system. The $Al_{0.3}Ga_{0.7}N$ (40 nm)/*i*-GaN (140 nm) thin films including the MSL were regrown with the *ex situ* process for the HEMTs. There were two types of samples grown in this study, as shown in Supplementary Figure S1: (A) HEMT structures on a sapphire substrate with various LT-GaN techniques for the *C*–*V* measurement using a Hg-probe tool and (B) the same structures on a GaN substrate for the device characteristics of lateral HEMTs. Figure 1A shows a schematic illustration of $Al_{0.3}Ga_{0.7}N$/*i*-GaN with LT-GaN MSLs regrown on the *p*-GaN layer. First, two *p*-GaNs with different Mg doping concentrations (1.0E19 and 4.0E19 cm^{-3}) were grown on sapphire substrates. After that, two types of the MSL, CLT-GaN and PLT-GaN, were introduced to investigate Mg out-diffusion

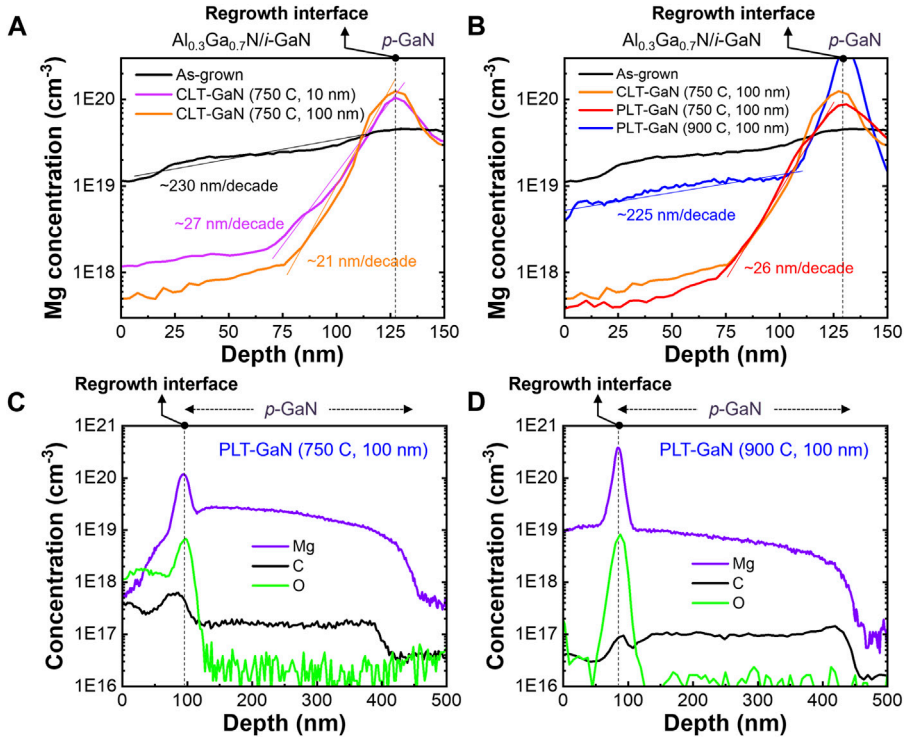

FIGURE 2
SIMS depth profiles to evaluate Mg out-diffusion decay rates in $Al_{0.3}Ga_{0.7}N$/*i*-GaN. **(A)** Thickness dependency of the CLT-GaN MSL. **(B)** Temperature dependency of the PLT-GaN MSL and SIMS depth profiles of Mg, C, and O for the 100-nm-thick PLT-GaN regrown at **(C)** 750°C and **(D)** 900°C. The fitting lines for extracting the Mg suppression rate are overlapped with the actual SIMS results.

TABLE 1 MOCVD growth conditions for LT-GaN MSLs.

MSL	Temperature	Thickness	Mg concentration of p-GaN
As-grown	-	-	1E19 or 4E19 cm^{-3}
CLT	750°C	10 nm	
	750°C	100 nm	
PLT	750°C	10 nm	
	750°C	100 nm	
	800°C	100 nm	
	850°C	100 nm	
	900°C	100 nm	

Two types of MSL (CLT- and PLT-GaNs) were regrown at the temperature region from 750°C to 900°C. The thickness of the LT-GaN MSLs was selected as 10 or 100 nm. 300-nm-thick *p*-GaNs with Mg concentrations of 1.0E19 or 4.0E19 cm^{-3} were prepared for the $Al_{0.3}Ga_{0.7}N$/*i*-GaN regrowth with these LT-GaN MSLs.

from *p*-GaN. The CLT-GaN MSL was regrown under a growth pressure of 600 mbar at 750°C with a consistent flow rate of TMGa and NH_3 sources into a H_2 atmospheric MOCVD reactor. Meanwhile, 50 cycles of (*i*) TMGa interruption (5 s) and (*ii*) TMGa injection (3 s) were implemented for the PLT-GaN MSL at the same growth pressure and temperature as the CLT-GaN MSL. Figure 1B shows the *in situ* reflectance and growth temperature during the MOCVD process for the $Al_{0.3}Ga_{0.7}N$/*i*-GaN/PLT-GaN thin-film regrowth on *p*-GaN. The part of the PLT-GaN growth step in Figure 2B is shown enlarged in Figure 1C, where two different growth rates repeated 50 times in one cycle can be observed: (i) a TMGa interruption step (5 s) and (ii) a TMGa injection step (3 s). On the other hand, the growth behavior of CLT-GaN is continuous. To investigate the suppression of Mg out-diffusion by applying these LT-GaN MSLs, the MOCVD growth temperature and thickness of LT-GaN were controlled as summarized in Table 1. Subsequent regrowth was conducted for 140-nm-thick *i*-GaN and 40-nm-thick $Al_{0.3}Ga_{0.7}N$ at 1,025°C and 1,080°C, respectively, to form the 2DEG structure. An XRD 2theta-omega scan of samples was performed, as shown in Supplementary Figure S6. For device fabrication, the mesa

etching was performed using a dry etching process with inductively coupled plasma reactive ion etching (ICP-RIE). For the source electrodes, Ti, Al, Ni, and Au were deposited on $Al_{0.3}Ga_{0.7}N$ followed by post-annealing using a rapid thermal annealing (RTA) system at 850°C for 45 s to form ohmic contacts. Al_2O_3 (12 nm thick) was deposited as a gate dielectric through atomic layer deposition (ALD). Ni/Au was deposited for the formation of the gate contact.

3 Results and discussion

Supplementary Figure S2 shows the AFM images of the grown 2DEG channel layer on sapphire substrates. RMS roughness shows significant differences between CLT- (~1.4 nm) and PLT LT-GaN (~0.40 nm). Figure 2 shows the SIMS depth profile for the regrown $Al_{0.3}Ga_{0.7}N$/*i*-GaN to evaluate Mg out-diffusion. The black dotted lines in Figure 2 indicate the *p*-GaN borderline or the place where the regrowth of $Al_{0.3}Ga_{0.7}N$/*i*-GaN with the MSL starts. The fitting lines for extracting the Mg suppression rate are overlapped with the actual SIMS results. For the as-grown sample without MSL (Figure 2A), the decay rate of Mg diffusion in the regrown $Al_{0.3}Ga_{0.7}N$/*i*-GaN region was estimated to be ~230 nm/decade. This result generally shows the diffusivity of Mg into regrown thin films on *p*-GaN. On the other hand, 10-nm-thick CLT-GaN as an MSL dramatically reduces the Mg diffusion rate (~27 nm/decade) in a regrown film. It was also found that CLT-GaN with a thickness of 100 nm further reduces Mg diffusion to ~21 nm/decade. The lowest Mg concentrations at 150-nm thicknesses of the regrown $Al_{0.3}Ga_{0.7}N$/*i*-GaN layer were 6.69E18 cm^{-3} for as-grown, 9.75E17 cm^{-3} for 10-nm-thick CLT-GaN grown at 750°C, and 5.94E17 cm^{-3} for 100-nm-thick CLT-GaN grown at 750°C. As Agarwal et al. (2017) previously reported, the PLT-GaN MSL regrown on *p*-GaN not only improves surface morphology but also suppresses Mg out-diffusion. Figure 2B shows that the 100-nm-thick PLT-GaN MSL grown at 750°C has a similar Mg suppression rate (~26 nm/decade) compared to the CLT-GaN MSL under the same growth conditions, but the lowest Mg concentration at 150 nm is reduced by almost half (3.67E17 cm^{-3}). Generally, these LT growth methods introduce various crystallography defects as well as impurities (C, O, and H) from byproducts of organic sources. The regrowth at a temperature lower than 750°C showed poor crystallinity of the thin films (not shown in this study) regardless of Mg suppression. For the other case, when the growth temperature is increased from 750°C to 900°C, 100-nm-thick PLT-GaN loses most of its role as the MSL, which indicates that Mg diffusion is very sensitive to the *p*-GaN surface temperature. Additionally, SIMS measurements, as shown in Figures 2C, D, obviously displayed the influence of growth temperature for the LT-GaN MSLs on the impurity concentration and the suppression of Mg diffusion. The concentration of O and C in the regrown $Al_{0.3}Ga_{0.7}N$/*i*-GaN layer decreases by more than one order of magnitude as the growth temperature of the MSL increases up to 900°C, but the suppression of Mg diffusion is significantly reduced. Since the impurity level strongly depends on the growth temperature, the impurities contained when inserting CLT-GaN and PLT-GaN grown at the same temperature are similar. Because of this reciprocal relationship, further studies on the LT-GaN MSL are required to simultaneously achieve Mg diffusion suppression and impurity reduction.

To investigate the 2DEG characteristics of regrown $Al_{0.3}Ga_{0.7}N$/*i*-GaN, the *C–V* measurement was obtained, as shown in Figure 3. Figure 3A shows the simulated energy band diagram of our $Al_{0.3}Ga_{0.7}N$/*i*-GaN. Bandgaps and offset values were obtained by the Silvaco TCAD (Sharbati et al., 2021). The calculated ΔE_c and ΔE_v were 377 and 171 meV, respectively. As shown in Figure 3B, the *C–V* measurements were directly obtained from the unprocessed samples at 1 MHz using a mercury (Hg)-probe system (MDC Model 802), which is commonly used for the *C–V* characterization of HEMTs without device fabrication (Cordier et al., 2008; Tucker et al., 2022). The Hg *C–V* system provides a non-destructive electrical characterization and employs a unique dot-ring configuration by forming a Schottky contact (dot contact) and an ohmic contact (ring contact) with the non-metalized planar semiconductor surface (Enisherlova et al., 2008). The *C–V* profiles show the measured capacitance with the bias voltage on the Schottky contact swept from 1 to −10 V, and the 2DEG sheet carrier density is calculated using the following equation (Kakanakova-Georgieva et al., 2007): $n_s = \left({}^{1}/_{qA}\right)\int C\,dV$, where q, A, C, and V are the elementary charge of electron (1.6E-19 coulomb), contact area (~4.57E-3 cm^{-2}), capacitance, and bias voltage, respectively. For data accuracy, the background capacitance value in *C–V* curves was removed, as shown in the Supplementary Material. The 2DEG density of $Al_{0.3}Ga_{0.7}N$/*i*-GaN regrown on a 300-nm-thick *i*-GaN without the LT-GaN MSLs was 4.27E12 cm^{-2} (the black curve in Figure 3). When 300-nm-thick *p*-GaN with Mg doping concentrations of 1.0E19 and 4.0E19 cm^{-3} was introduced, the 2DEG density abruptly decreased to 2.84E10 and 1.76E10 cm^{-2}, respectively, as shown in Figure 3C. This result indicates that the 2DEG is damaged by the Mg diffusion into $Al_{0.3}Ga_{0.7}N$/*i*-GaN. Figure 3D shows that the 2DEG density of $Al_{0.3}Ga_{0.7}N$/*i*-GaN slightly improved by 5.21E10 cm^{-2} when 10-nm-thick CLT-GaN regrown at 750°C was inserted onto *p*-GaN (Mg: 4.0E19 cm^{-3}). As the thickness of CLT-GaN was increased to 100 nm (Figure 3E), the 2DEG density increased noticeably to 1.58E12 and 4.39E11 cm^{-2} when the Mg doping concentrations of *p*-GaN were 1.0E19 and 4.0E19 cm^{-3}, respectively. To improve the crystallinity and surface properties of regrown $Al_{0.3}Ga_{0.7}N$/*i*-GaN thin films, PLT-GaN was also introduced as the MSL (Figure 3F). With the reduction in the growth temperature from 900°C to 750°C for 100-nm-thick PLT-GaN, the 2DEG density of $Al_{0.3}Ga_{0.7}N$/*i*-GaN regrown on *p*-GaN (Mg: 4.0E19 cm^{-3}) increased from 1.74E11 to 3.13E12 cm^{-2}. This is due to the increased suppression efficiency against Mg diffusion in accordance with lowering the growth temperature of MSLs, which could be easily inferred from the SIMS results (Figure 2B). The efficacy of PLT-GaN to suppress Mg diffusion also depends on its thickness. As shown in Figures 3G, H, the 2DEG density increased significantly when the thickness of the PLT-GaN was increased from 10 to 100 nm. With the 100-nm-thick PLT-GaN grown at 750°C, the highest 2DEG density of $Al_{0.3}Ga_{0.7}N$/*i*-GaN regrown on *p*-GaN (Mg: 1.0E19 cm^{-3}) was 4.04E12 cm^{-2}, which should be related to the crystalline quality of regrown thin films with the PLT growth method. It is worth mentioning that our previous bandgap simulation result showed different electron densities in 2DEG according to the Mg diffusion into the $Al_{0.3}Ga_{0.7}N$/*i*-GaN

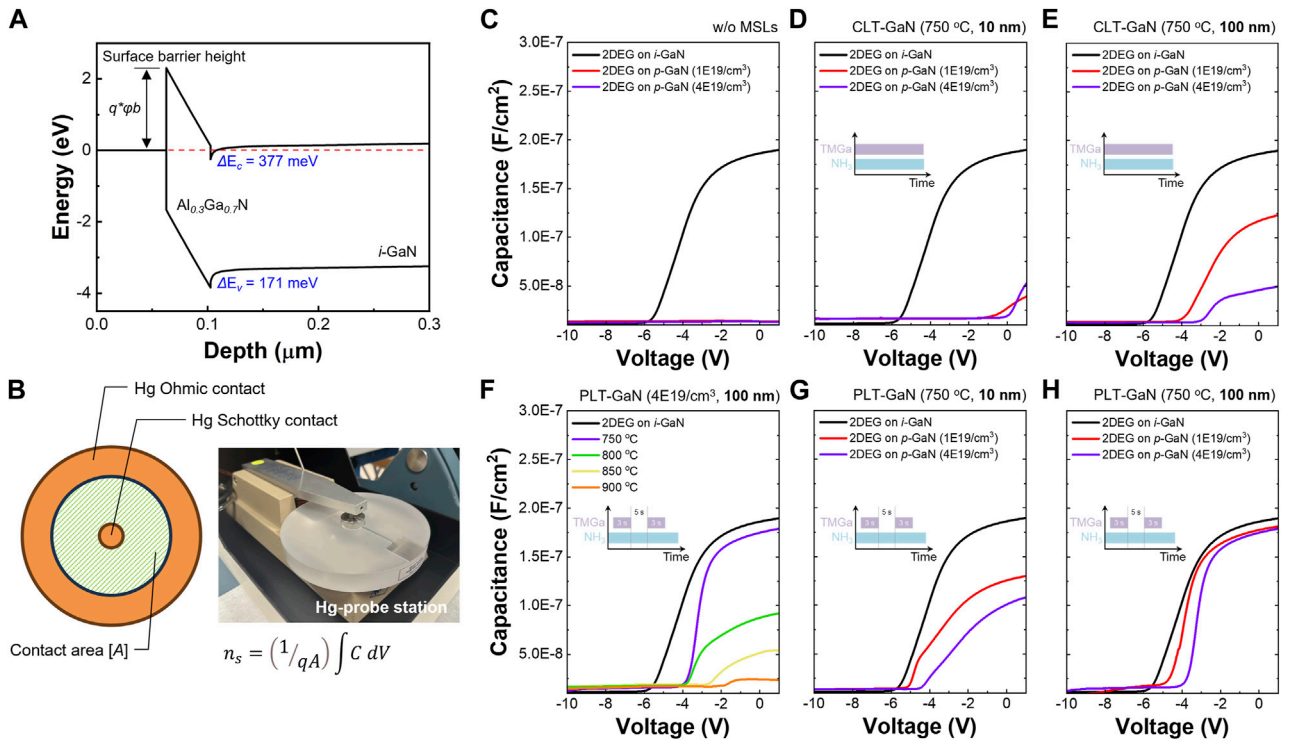

FIGURE 3
(A) Energy band diagram of our $Al_{0.3}Ga_{0.7}N$/*i*-GaN. **(B)** Photograph of the contactless Hg-probe station with schematics of a contact area for the measurement of 2DEG density. **(C–H)** *C–V* results of $Al_{0.3}Ga_{0.7}N$/*i*-GaN regrown on *p*-GaN with various MOCVD growth conditions of MSLs. The 2DEG density was extracted from the *C–V* curves.

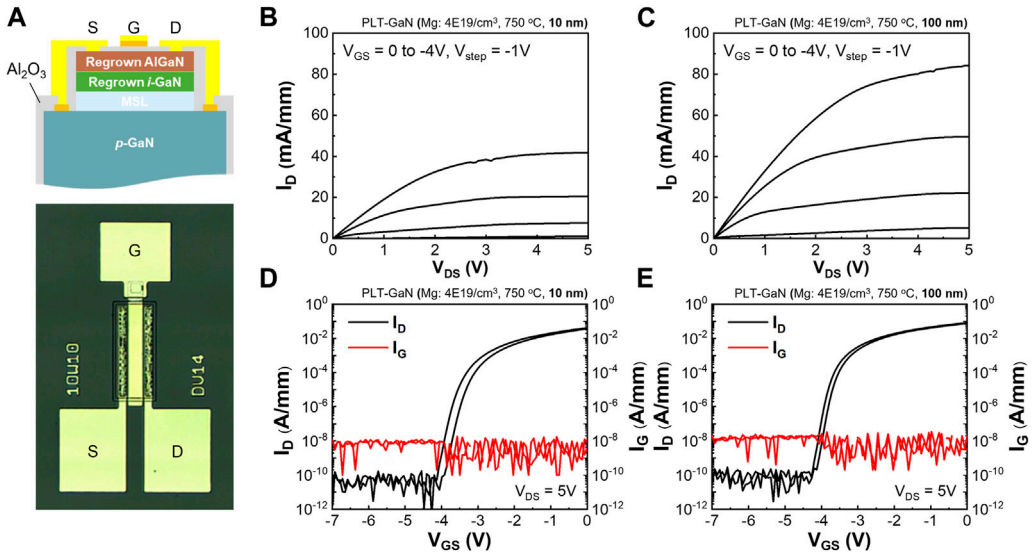

FIGURE 4
(A) Cross-section schematics and the plan-view optical microscope image of the lateral HEMT. I_D–V_{DS} measurement of lateral HEMTs on *p*-GaN using **(B)** 10-nm-thick and **(C)** 100-nm-thick PLT-GaNs as the MSL. Transfer characteristics of lateral HEMTs on *p*-GaN using **(D)** 10-nm-thick and **(E)** 100-nm-thick PLT-GaNs as the MSL.

regrown on *p*-GaN (Lee et al., 2022). Additionally, we confirmed that there was no significant difference in *C*–*V* results before and after *p*-GaN activation, indicating that the electron density of 2DEG formed on *p*-GaN changes more sensitively depending on the degree of Mg diffusion than *p*-GaN activation (details not shown).

Figure 4 presents the output and transfer characteristics of the fabricated lateral HEMTs regrown on *p*-GaN with 10- and 100-nm-thick PLT-GaN MSLs. Figure 4A shows the cross-section device schematics and the plan-view optical microscope image. In the case of HEMTs without the MSL, no 2DEG characteristics were observed (not shown). The gate voltage was swept from 0 to −4 in −1 V steps. The threshold voltage (V_{th}) was defined as the gate voltage (V_G) when the drain current reaches 1 mA/mm at a drain bias of 5 V from the I_D–V_{GS} curve (Hwang et al., 2013). The on-state resistance is extracted from the gradient of I_D–V_{DS} curves at V_{GS} = 0 V and V_{DS} from 0 to 0.5 V. A maximum drain current density (I_{max}) increases from 41.5 to 84.5 mA/mm as the thickness of the PLT-GaN MSL increases, as shown in Figures 4B, C. The I_D–V_{GS} hysteresis was 0.21 and 0.14 V for the 10-nm- and 100-nm-thick MSL, respectively. From the SIMS and *C*–*V* analysis, it is shown that increasing the thickness of PLT-GaN MSLs could further suppress the Mg diffusion into the 2DEG. Therefore, I_{max} can be increased by maintaining a high-electron density in the 2DEG region. The V_{th} of these HEMTs is −4.12 V, and the on-state resistance is 52 and 31 mΩ·mm with 10- and 100-nm-thick PLT-GaN, respectively. The I_D–V_{GS} transfer characteristics show well-behaved curves, as plotted in Figures 4D, E. The average gate leakage (I_G) of HEMTs using 10- and 100-nm-thick PLT-GaNs was similar to ~1.45E-8 A/mm. The I_D off-current representing the leakage current characteristics related to defects was 5.74E-11 and 5.36E-11 A/mm, respectively, in the case of using 10- and 100-nm-thick PLT-GaNs. The two values do not show a large difference, and when PLT is used, defect density, one of the main issues of LT-GaN growth, shows no sensitivity according to the thickness of PLT-GaN. The subthreshold slopes were also calculated as 99.23 and 83.19 mV/dec for the 10- and 100-nm-thick MSLs, respectively.

4 Conclusion

We addressed the PLT-GaN and CLT-GaN inserted between $Al_{0.3}Ga_{0.7}N$/*i*-GaN and *p*-GaN to suppress Mg out-diffusion. In SIMS depth profiling, PLT-GaN improved the Mg decay rate up to ~21 nm/decade in regrown $Al_{0.3}Ga_{0.7}N$/*i*-GaN on *p*-GaN, presenting a much higher decay rate compared to the case without any suppression layers (~230 nm/decade). In addition, the *C*–*V* characteristic showed a high electron density of 3.13E12 cm^{-2} in 2DEG of $Al_{0.3}Ga_{0.7}N$/*i*-GaN with the PLT-GaN MSL on *p*-GaN (Mg: 4.0E19 cm^{-3}), which is the almost same electron concentration (4.27E12 cm^{-2}) as that in 2DEG grown without *p*-GaN. In addition, we successfully demonstrated the electrical characteristics of the lateral HEMTs regrown on *p*-GaN with 10- and 100-nm-thick PLT-GaN MSLs. This study provides a pathway to solve a critical bottleneck caused by Mg out-diffusion and enables diverse applications in high-efficiency and high-output power electronics that require GaN-based epi-structures embedding *p*-GaN layers.

Data availability statement

The raw data supporting the conclusion of this article will be made available by the authors, without undue reservation.

Author contributions

SC and KL designed and discussed the experiments. KL grew GaN-based thin films by using the MOCVD system. YN and JC designed the devices. XW, YN, and JC fabricated and analyzed the HEMT devices. KL and MN analyzed the SIMS results. CM analyzed *C*–*V* results. All authors contributed to the article and approved the submitted version.

Funding

The authors gratefully acknowledge the financial support provided by ONR grant N00014-21-1-2167, supervised by. Mr. (Ret. Capt.) Lynn Petersen.

Conflict of interest

The authors declare that the research was conducted in the absence of any commercial or financial relationships that could be construed as a potential conflict of interest.

Publisher's note

Supplementary material

The Supplementary Material for this article can be found online at: https://www.frontiersin.org/articles/10.3389/fmats.2023.1229036/full#supplementary-material

References

Agarwal, A., Tahhan, M., Mates, T., Keller, S., and Mishra, U. (2017). Suppression of Mg propagation into subsequent layers grown by MOCVD. *J. Appl. Phys.* 121, 25106. doi:10.1063/1.4972031

Benzarti, Z., Halidou, I., Bougrioua, Z., Boufaden, T., and El Jani, B. (2008). Magnesium diffusion profile in GaN grown by MOVPE. *J. Cryst. Growth* 310, 3274–3277. doi:10.1016/j.jcrysgro.2008.04.008

Brown, D. F., Shinohara, K., Corrion, A. L., Chu, R., Williams, A., Wong, J. C., et al. (2013). High-speed, enhancement-mode GaN power switch with regrown ${\rm n}+ $ GaN ohmic contacts and staircase field plates. *IEEE electron device Lett.* 34, 1118–1120. doi:10.1109/led.2013.2273172

Chowdhury, S., and Mishra, U. K. (2013). Lateral and vertical transistors using the AlGaN/GaN heterostructure. *IEEE Trans. Electron Devices* 60, 3060–3066. doi:10.1109/ted.2013.2277893

Chowdhury, S., Swenson, B. L., and Mishra, U. K. (2008). Enhancement and depletion mode AlGaN/GaN CAVET with Mg-ion-implanted GaN as current blocking layer. *IEEE Electron Device Lett.* 29, 543–545. doi:10.1109/led.2008.922982

Chowdhury, S., Swenson, B. L., Wong, M. H., and Mishra, U. K. (2013). Current status and scope of gallium nitride-based vertical transistors for high-power electronics application. *Semicond. Sci. Technol.* 28, 074014. doi:10.1088/0268-1242/28/7/074014

Chowdhury, S., Wong, M. H., Swenson, B. L., and Mishra, U. K. (2011). CAVET on bulk GaN substrates achieved with MBE-regrown AlGaN/GaN layers to suppress dispersion. *IEEE Electron Device Lett.* 33, 41–43. doi:10.1109/led.2011.2173456

Cordier, Y., Moreno, J.-C., Baron, N., Frayssinet, E., Chenot, S., Damilano, B., et al. (2008). Demonstration of AlGaN/GaN high-electron-mobility transistors grown by molecular beam epitaxy on Si (110). *IEEE electron device Lett.* 29, 1187–1189. doi:10.1109/led.2008.2005211

Enisherlova, K. L., Gulyaev, I. B., Goryachev, V. G., Dorofeev, A. U., Temper, E. M., and Gladisheva, N. B. (2008). "AlxGa (1-x) N/GaN structure diagnostic by CV characteristics method," in *Micro-and nanoelectronics 2007* (Bellingham, Washington, USA: SPIE), 321–328.

Fichtenbaum, N. A., Mates, T. E., Keller, S., DenBaars, S. P., and Mishra, U. K. (2008). Impurity incorporation in heteroepitaxial N-face and Ga-face GaN films grown by metalorganic chemical vapor deposition. *J. Cryst. Growth* 310, 1124–1131. doi:10.1016/j.jcrysgro.2007.12.051

Hwang, I., Kim, J., Choi, H. S., Choi, H., Lee, J., Kim, K. Y., et al. (2013). p-GaN gate HEMTs with tungsten gate metal for high threshold voltage and low gate current. *IEEE Electron Device Lett.* 34, 202–204. doi:10.1109/led.2012.2230312

Kakanakova-Georgieva, A., Forsberg, U., Ivanov, I. G., and Janzén, E. (2007). Uniform hot-wall MOCVD epitaxial growth of 2 inch AlGaN/GaN HEMT structures. *J. Cryst. Growth* 300, 100–103. doi:10.1016/j.jcrysgro.2006.10.242

Lee, K. J., Nakazato, Y., Chun, J., Wen, X., Meng, C., Soman, R., et al. (2022). Nanoporous GaN on p-type GaN: a Mg out-diffusion compensation layer for heavily Mg-doped p-type GaN. *Nanotechnology* 33, 505704. doi:10.1088/1361-6528/ac91d7

Lee, Y.-J., Yao, Y.-C., Huang, C.-Y., Lin, T.-Y., Cheng, L.-L., Liu, C.-Y., et al. (2014). High breakdown voltage in AlGaN/GaN HEMTs using AlGaN/GaN/AlGaN quantum-well electron-blocking layers. *Nanoscale Res. Lett.* 9, 433–439. doi:10.1186/1556-276x-9-433

Ran, J., Wang, X., Hu, G., Wang, J., Li, J., Wang, C., et al. (2006). Study on Mg memory effect in npn type AlGaN/GaN HBT structures grown by MOCVD. *Microelectron. J.* 37, 583–585. doi:10.1016/j.mejo.2005.10.001

Sharbati, S., Gharibshahian, I., Ebel, T., Orouji, A. A., and Franke, W.-T. (2021). Analytical model for two-dimensional electron gas charge density in recessed-gate GaN high-electron-mobility transistors. *J. Electron. Mater.* 50, 3923–3929. doi:10.1007/s11664-021-08842-7

Soman, R., Raghavan, S., and Bhat, N. (2019). An *in situ* monitored and controlled etch process to suppress Mg memory effects in MOCVD GaN growth on Si substrate. *Semicond. Sci. Technol.* 34, 125011. doi:10.1088/1361-6641/ab5006

Tomita, K., Itoh, K., Ishiguro, O., Kachi, T., and Sawaki, N. (2008). Reduction of Mg segregation in a metalorganic vapor phase epitaxial grown GaN layer by a low-temperature AlN interlayer. *J. Appl. Phys.* 104, 14906. doi:10.1063/1.2952051

Tucker, E., Ramos, F., Frey, S., Hillard, R. J., Horváth, P., Zsákai, G., et al. (2022). Characterization of $Al_{<i>X</i>}Ga_{1-<i>X</i>}N$/GaN high electron mobility transistor structures with mercury probe capacitance–voltage and current–voltage. *Phys. status solidi* 219, 2100416. doi:10.1002/pssa.202100416

Wu, Y., Liu, B., Xu, F., Sang, Y., Tao, T., Xie, Z., et al. (2021). High-efficiency green micro-LEDs with GaN tunnel junctions grown hybrid by PA-MBE and MOCVD. *Photonics Res.* 9, 1683–1688. doi:10.1364/prj.424528

Xiao, M., Zhang, R., Dong, D., Wang, H., and Zhang, Y. (2019). Design and simulation of GaN superjunction transistors with 2-DEG channels and fin channels. *IEEE J. Emerg. Sel. Top. Power Electron.* 7, 1475–1484. doi:10.1109/jestpe.2019.2912978

Xing, H., Green, D. S., Yu, H., Mates, T., Kozodoy, P., Keller, S., et al. (2003). Memory effect and redistribution of Mg into sequentially regrown GaN layer by metalorganic chemical vapor deposition. *Jpn. J. Appl. Phys.* 42, 50–53. doi:10.1143/jjap.42.50

Zhou, Q., Huang, P., Shi, Y., Chen, K., Wei, D., Zhu, R., et al. (2019). A novel kilovolts GaN vertical superjunction MOSFET with trench gate: approach for device design and optimization. *IEEE J. Emerg. Sel. Top. Power Electron.* 7, 1440–1448. doi:10.1109/jestpe.2019.2924333